International Journal of Heat and Mass Transfer 54 (2011) 739–745

Contents lists available at ScienceDirect

International Journal of Heat and Mass Transfer

journal homepage: www.elsevier.com/locate/ijhmt

Technical Note

Dry-out CHF correlation for R134a flow boiling in a horizontal helically-coiled tube

C.N. Chen [a,b], J.T. Han [a], T.C. Jen [b,*], L. Shao [a]

[a] School of Energy and Power Engineering, Shandong University, Jinan, Shandong Province 250061, PR China
[b] Department of Mechanical Engineering, University of Wisconsin-Milwaukee, Milwaukee, WI 53201, USA

ARTICLE INFO

Article history:
Received 3 February 2010
Received in revised form 18 August 2010
Accepted 18 August 2010
Available online 12 October 2010

Keywords:
Dry-out CHF
Horizontal helically-coiled tubes
Boiling heat transfer
R134a

ABSTRACT

An experimental study was carried out to investigate the R134a dry-out critical heat flux (CHF) characteristics in a horizontal helically-coiled tube. The test section was heated uniformly by DC high-power source, and its geometrical parameters are the outer diameter of 10 mm, inner diameter of 8.4 mm, coil diameter of 300 mm, helical pitch of 75 mm and valid heated length of 1.89 m. The experimental parameters are the outlet pressures of 0.30–0.95 MPa, mass fluxes of 60–500 kg m^{-2} s^{-1}, inlet qualities of −0.36–0.35 and heat fluxes of 7.0×10^3–5.0×10^4 W m^{-2}. A method based on Agilent BenchLink Data Logger Pro was developed to determine the occurrence of CHF with a total of 68 T-type thermocouples (0.2 mm) set along the tube for accurate temperature measurement. The characteristics of wall temperatures and the parametric effect on dry-out CHF showed that temperature would jump abruptly at the point of CHF, which usually started to form at the front and offside (270° and 90°) of the outlet cross-section. The CHF values decrease nearly linearly with increasing inlet qualities, while they decrease more acutely with increasing critical qualities, especially under larger mass flux conditions. The mass flux has a positive effect on CHF enhancement, but the pressure has negative one. A new dimensionless correlation was developed to estimate dry-out CHF of R134a flow boiling in horizontal helically-coiled tubes under current experimental conditions and compared to calculated results from Bowring and Shah correlations.

1. Introduction

Critical heat flux (CHF) is one of the most significantly monitored parameters for operating heating equipment such as refrigeration evaporator, once-through boiler, and nuclear reactor bundles. Under the uniformly heating condition, the heat transfer coefficient will decrease suddenly and the heated wall temperature increases abruptly when CHF occurs [1]. Without effective control, the wall temperature will exceed the maximum temperature of materials, damaging the heating facilities and possibly endangering those who are operating the equipment. Because of the importance of CHF to engineering applications, thousands of researchers have developed more than one thousand correlations and hundreds of methods for estimating CHF in the past four decades, including theory analysis and experimental investigations [2–11]. Although successful approaches such as fluid to fluid modeling [2], look-up table (LUT) [3] and neural network forecasting [4] are widely used, no one has been able to reveal the causes of CHF due to its complicated mechanism, especially in complex flow channels. Since there is no universal method for investigating particular situations, specific experiment investigation is still considered to be the best way to reveal the cause of CHF.

Based on two main different theoretical explanations for the CHF trigger mechanism in different conditions, CHF is generally classified into two types named DNB (departure from nucleate boiling) CHF and dry-out CHF, respectively. The former, which is more suited toward nuclear reactors, usually occurs under much higher heat flux than the later. For general industry processes dry-out CHF is more frequently used and often results in accidents. Therefore, studying the characteristics of dry-out CHF is a necessary to ensure the safety of the heat transfer process.

Much previous work mainly focused on the CHF in straight tubes with various fluids. Bowring [5] developed a correlation for dry-out heat flux in round tube using water as working fluid based on 3800 experimental data over the pressure range 0.7–12 MPa, with an error of 7% for CHF in water; Ahmad [2] suggested the famous compensated distortion model for fluid to fluid modeling of CHF, which could be applied for CFCs, CO_2 and potassium; Katto and Ohno [6] investigated on CHF of forced convective boiling in uniformly heated vertical tubes. Their experiments covered nearly all the regimes of CHF, but concerned only about vertical tubes; Shah [7] improved general correlation for upstream flow CHF in vertical tubes. His new correlation greatly agreed with CHF data of 23 fluids from 62 independent sources. Therefore, it was one

* Corresponding author. Tel.: +1 414 229 2307; fax: +1 414 229 6958.
E-mail address: jent@uwm.edu (T.C. Jen).

0017-9310/$ - see front matter © 2010 Elsevier Ltd. All rights reserved.
doi:10.1016/j.ijheatmasstransfer.2010.09.027

Nomenclature

A	heated area of the test section (m^2)
B_o	boiling number $B_o = \frac{q_{cr}}{G \cdot \gamma}$
C_p	thermal capacity (J kg^{-1} K^{-1})
D	hydraulic diameter (m)
D_c	coil diameter (m)
D_n	Dean number $D_n = \mathrm{Re}\left(\frac{D}{D_c}\right)^{0.5}$
G	mass flux (kg m^{-2} s^{-1})
I	current (A)
L	heated length (m)
N_d	liquid-gas density ratio $N_d = \frac{\rho_l}{\rho_g}$
P	pressure (MPa)
P_A	power value logged by Agilent BenchLink Data Logger Pro (W)
P_e	power supplies for test section (W)
P_p	power supplies for preheating section (W)
q_{cr}	critical heat flux (W m^{-2})
Re	Reynolds number $\mathrm{Re} = \frac{GD}{\mu}$
r_i	inner radius of the test tube (m)
r_o	outer radius of the test tube (m)
S	section symbol of the test tube
T_0	temperature rise of an empty tube as same as the test section with increasing heat flux δq (K)
T_i	temperature at time i (°C)
T_{i-1}	temperature at time i − 1 (°C)
T_w	wall temperature (°C)
U	voltage (V)
x_{cr}	critical quality
x_i	inlet quality
x_o	outlet quality

Greek symbols

γ	latent heat of evaporation (J kg^{-1})
Δh_i	inlet subcooling enthalpy (J kg^{-1})
δq	increment of heat flux (W m^{-2})
δT	temperature difference value defined according to experimental conditions (K)
δt	error of T-type thermocouples (K)
μ	dynamic viscosity (Pa s)
ρ	density (kg m^{-3})

Subscripts

exp	experimental data
g	gas phase
l	liquid phase
pre	prediction data
ss	stainless steel

of the most extensively used CHF correlations; Wong et al. [8] also devised a new forecasting method for horizontal straight tubes; Tain and Cheng [9] studied CHF in round tube for CFCs and CFC alternatives; Kim et al. [10] investigated the CHF in water with vertical tubes at low pressure and low flow conditions (LPLF). They compared parametric trends under these special conditions with previous general understandings, considering the complex effects of system pressure and tube diameter; Pioro et al. [11] compared the R134a CHF data in vertical tubes with the water CHF look-up table; Kim and Chang [12] performed an experimental study on CHF in uniformly heated vertical tube using R134a; Groeneveld et al. [3] updated the CHF look-up table, which was a normalized data bank for vertical 8 mm water-cooled tube based on more than 30,000 data points; Sindhuja et al. [13] studied mixture R407c CHF in vertical tubes and compared the results with pure fluids, finding that the CHF characteristics change due to the mixture properties changing along the boiling length, but the results still showed lower CHF at higher pressure conditions as in the case of pure fluids. In addition, some efforts were contributed to investigate the CHF in nuclear reactor bundles [14–19]. Review of the previous work shows that those studies were mainly related to CHF behaviors in straight tubes, or bundles concerned by nuclear reactor only, using water which required high pressure and temperature or some CFCs which are toxic to the environment.

The helically-coiled tube has been widely used in energy engineering and petrochemical industry since it has enhanced heat transfer properties [20]. Compared to straight tube, it has the advantage of high heat transfer efficiency and compact structure. When oriented horizontally, the tube can have a greater heat transfer area than that of a straight tube in the same amount of space. It is especially true for applications in aircrafts and submarines, which both have limited space to operate in and the tube should be placed horizontally with a lower gravity center. Due to the special coiled structure, the CHF characteristics in this kind of tube are different from straight one, which should be studied. In this study, to avoid the high latent heat of water and the destruction to the ozone layer by CFCs, experiments were performed using R134a to develop correlations for predicting dry-out CHF in horizontal helically-coiled tubes.

2. Experimental apparatus and procedure

2.1. Experimental circle loop

The experimental set-up consists of two circle loops, the working loop (R134a) and the cooling loop (30% $Cacl_2$ solution), as shown in Fig. 1. It includes the following components: canned motor pump, Coriolis mass flow-meter, preheating/test sections, precision DC power supplies, condenser, refrigeration chilling unit, N_2-gas accumulator and data acquisition system. The working loop is designed for pressure of 1.6 MPa and temperature of 200 °C, preheating section power of 24 V × 300 A and test section of 60 V × 500 A. The refrigeration chilling unit has a maximum output of 5.0×10^4 W.

2.2. Test section and installation

The test section is made of stainless steel tube (SUS304), as shown in Fig. 2. It has a 300 mm coil diameter and a 75 mm helical pitch and its outer diameter and inner diameter are 10 mm and 8.4 mm, respectively. The valid heated coiled length is 1.89 m. The test section is directly heated by high current DC power supplies to generate constant heat flux (ignoring resistance variation).

The temperatures of the working fluid R134a at the inlet and outlet of the test section are measured with 0.3 mm T-type sheathed thermocouples (copper-constantan). The precision pressure sensors are set at the same positions as thermocouples in order to measure the inlet and outlet pressures accurately. The temperatures of outside wall are measured by 68 T-type thermocouples (0.2 mm) set along the test tube. Eight symmetrical positions of each coil of the helically-coiled tube, i.e. every quarter-coil, as S1–S5 indicated in Fig. 2(a), are selected for the measuring sections where four thermocouples are set evenly around the

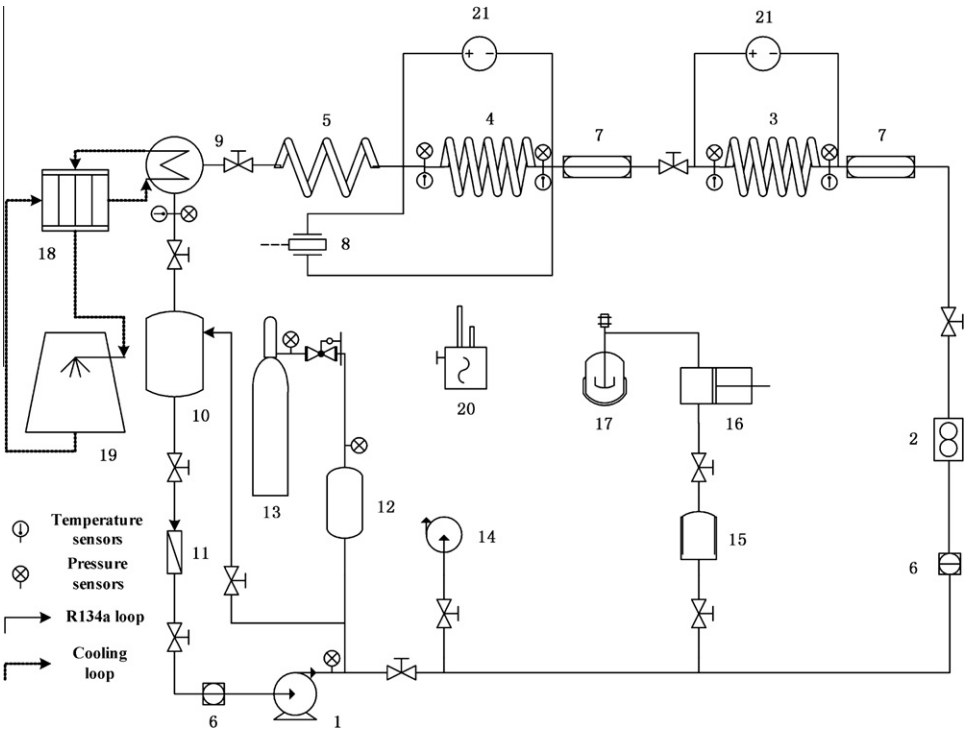

Fig. 1. Schematic diagram of the experimental circle loop. 1 motor pump, 2 Coriolis mass flow-meter, 3 preheating Section, 4 test Section, 5 flow pattern observing Section, 6 sight glass, 7 visual section, 8 differential pressure gage, 9 condenser, 10 receiver tank, 11 dry-strainer, 12 accumulator, 13 N_2 gas tank, 14 vacuum pump, 15 buffer tank, 16 refrigerant pump, 17 refrigerant tank, 18 chilling unit, 19 cooling tower, 20 halogens leak detector, 21 DC power supply.

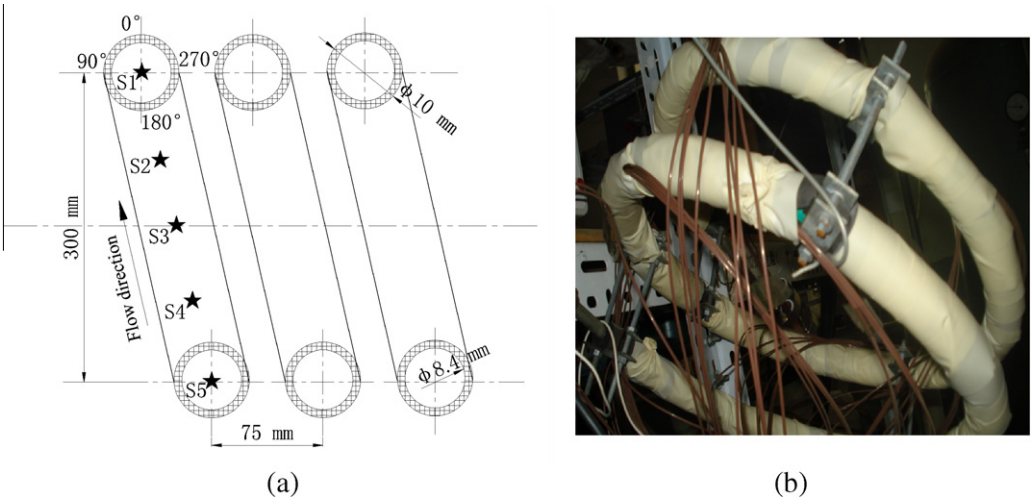

Fig. 2. Structure of the test tube and thermocouple installation.

circumferences, as 0°, 90°, 180° and 270° indicated in Fig. 2(a), which are named upside, offside, underside and front, respectively. The inlet section and the outlet section are both 5 mm away from the copper electrodes connected to DC power supplies. Three pairs of clamps are installed to stop from distortion of test tube, as indicated in Fig. 2(b). All the experimental signals are collected and processed by Agilent 34980A data acquisition system.

2.3. Experimental conditions and procedure

For the practical operation conditions of water-vapor in medium and low pressure boilers and heat exchangers, 2.0–6.0 MPa of pressure in water is approximately equivalent to 0.29–0.96 MPa in R134a at the same gas-liquid ratios. In order to collect data in this range and for the purpose of fluid-to-fluid modeling, the CHF experiments were carried out at pressures of 0.30–0.95 MPa, mass fluxes of 60–500 kg $m^{-2}s^{-1}$, inlet qualities of −0.36–0.35 and heat fluxes of 7.0×10^3–5.0×10^4 W m^{-2}. The working fluid is brand DuPont™ Suva® 134a, whose thermophysical properties are listed in Table 1.

The procedures were conducted as follows. The helically-coiled tube was placed horizontally and connected to the system with insulated flanges. Before each experiment, heat balance testing was performed and results showed that the heat loss was no more than 5%. R134a from the receiver tank is circulated through the whole system by canned motor pump. The mass flux can be

Table 1
Thermophysical properties of R134a used in experimental investigation.

No.	Items	Units	Properties
1	Brand name	–	DuPont™ Suva® 134a
2	Chemical formula	–	CH_2FCF_3
3	Molecular weight	–	102.03
4	Boiling point (1 atm)	°C	−26.06
5	Freezing point	°C	−103
6	Critical temperature	°C	101.08
7	Critical pressure	MPa	4.06
8	Critical density	kg m^{-3}	515.3
9	Critical volume	m^3 kg^{-1}	1.94×10^{-3}
10	Density (Liquid, 25 °C)	kg m^{-3}	1.21×10^{3}
11	Thermal capacity (Liquid, 25 °C)	J kg^{-1} K^{-1}	1.44×10^{3}
12	Vapor pressure (25 °C)	MPa	0.666
13	Latent heat of evaporation (Boiling point)	J kg^{-1}	217.2
14	Thermal conductivity (Liquid, 25 °C)	W m^{-1} K^{-1}	0.0824
15	Thermal conductivity (Gas, 1 atm)	W m^{-1} K^{-1}	0.0145
16	Viscosity (Liquid, 25 °C)	Pa s	2.02×10^{-4}
17	Viscosity (Gas, 1 atm)	Pa s	1.20×10^{-5}
18	Self-ignition temperature	°C	770
19	Ozone depletion potential (ODP)	–	0
20	Halocarbon global warming potential (HGWP)	–	0.28

adjusted according to the speed of motor and control valves. The pressure is controlled by adjusting mass flux of cooling loop, power supply to preheating section and N_2-gas accumulator. When the pressure and mass flux of the system are stabilized to predetermined values, the inlet temperature is controlled by increasing or decreasing power supply to preheating section. The power supply to test section is increased rapidly at the beginning, and then slowly at each step of around 50 W m^{-2} until CHF occurs. A method based on Agilent BenchLink Data Logger Pro was developed to determine the occurrence of CHF. Critical heat flux phenomena are considered to occur once any wall temperature T_i detected by thermocouples satisfies Eq. (1). Subsequently, the Agilent software sends signal to cut off power supplies within 0.1 s.

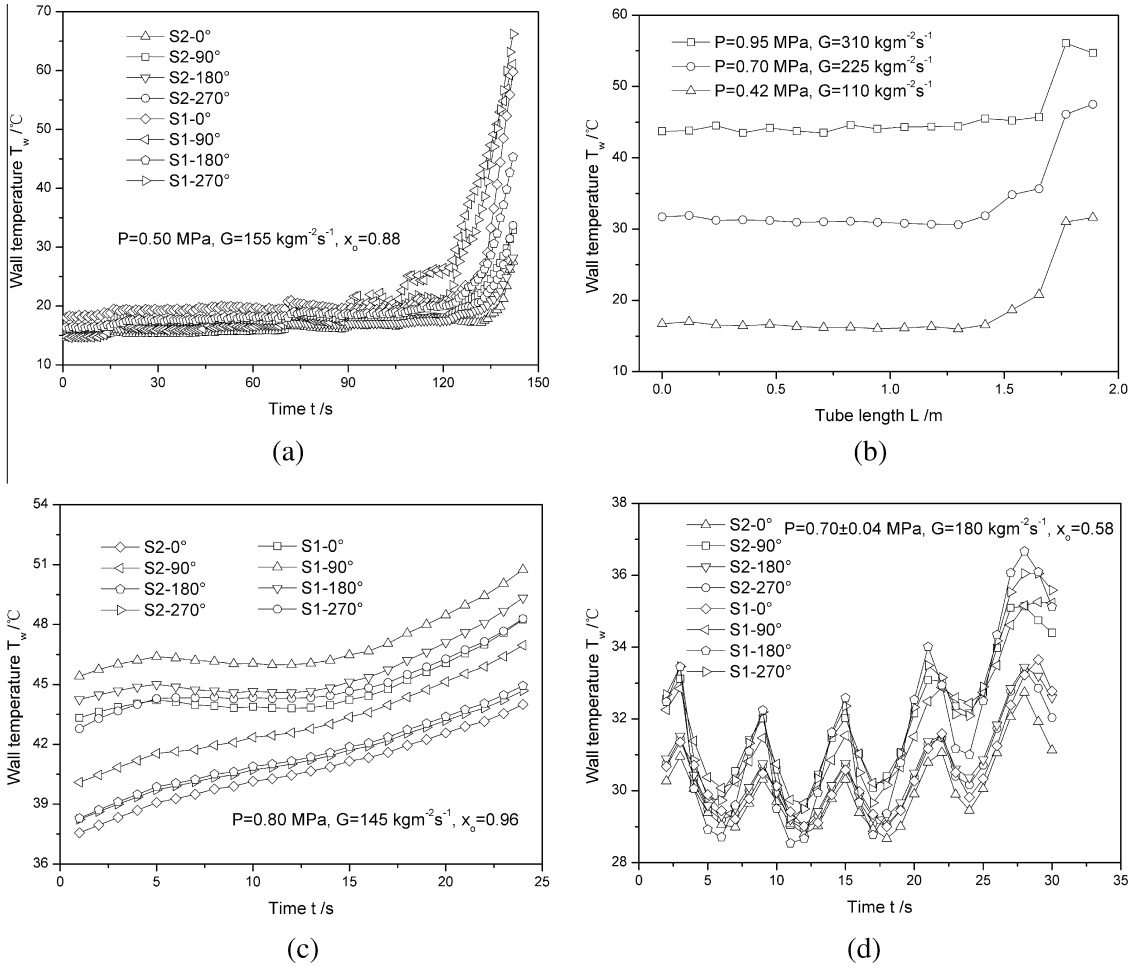

Fig. 3. Characteristics of wall temperature distribution under different conditions.

$$T_0 - (T_i - T_{i-1}) \leqslant \delta T + \delta t$$
$$T_0 = \frac{2 \cdot \delta q \cdot r_i}{(r_o^2 - r_i^2) \cdot \rho_{ss} \cdot C_{p,ss}} \quad (1)$$

3. Experimental results and discussion

3.1. Data reduction

In order to introduce the characteristics of CHF in horizontal helically-coiled tubes, critical heat flux q_{cr} (CHF value), inlet vapor quality x_i, outlet vapor quality x_o and critical vapor quality x_{cr} are needed. They are calculated as follows.

q_{cr} is derived from the arithmetic average of value q_{cr1} calculated by Agilent software and value q_{cr2} calculated by product of voltage U and current I logged in DC power supplies.

$$q_{cr} = \frac{q_{cr1} + q_{cr2}}{2}$$
$$q_{cr1} = \frac{P_A}{A}, \quad q_{cr2} = \frac{U \cdot I}{A} \quad (2)$$
$$A = 2\pi r_i L$$

Considering the heat loss of system within 5%, vapor qualities x_i, x_o and x_{cr} are evaluated by energy balance equation.

$$x_i = \frac{0.95P_p}{\pi \cdot G \cdot r_i^2 \cdot \gamma} - \frac{\Delta h_i}{\gamma}$$
$$x_o = x_i + \frac{0.95P_e}{\pi \cdot G \cdot r_i^2 \cdot \gamma} \quad (3)$$

Strictly speaking, when dry-out CHF happened, outlet of the test section has high vapor quality and the thermodynamic equilibrium has been broken [21]. However, calculating the real critical vapor quality is difficult. For the purpose of evaluating CHF, it is feasible to suppose the critical vapor quality x_{cr} equals the thermodynamic equilibrium outlet vapor quality x_o.

3.2. Characteristics of wall temperature distribution

Dry-out CHF usually starts at the outlet section near outlet copper electrode and spreads to the whole section circumference immediately; the wall temperature will then increase very quickly. For example, at 0.50 MPa and 155 kg m^{-2} s^{-1} the rise of temperatures of the two sections S1 and S2 at the end of test tube are shown in Fig. 3(a). They vary almost from 15 °C to 70 °C rapidly. And wall temperatures of S1 rise much earlier than those of S2. And the wall temperatures at the front and offside (270° and 90°) frequently are much higher than those of the other two sides. The locations of the sudden temperature rise along the heated length are shown in Fig. 3(b). The wall temperatures show the same abrupt increase along the heated length for different experimental conditions.

After the CHF occurs, all the wall temperatures sometimes will rise slowly and even decrease to some extent, as shown in Fig. 3(c), when there is a high outlet vapor quality. This refers to the steady dry-out area in which the heating facilities may not be immediately destroyed. On the contrary, the wall temperatures will show a fluctuating state with pressure wave when the outlet vapor

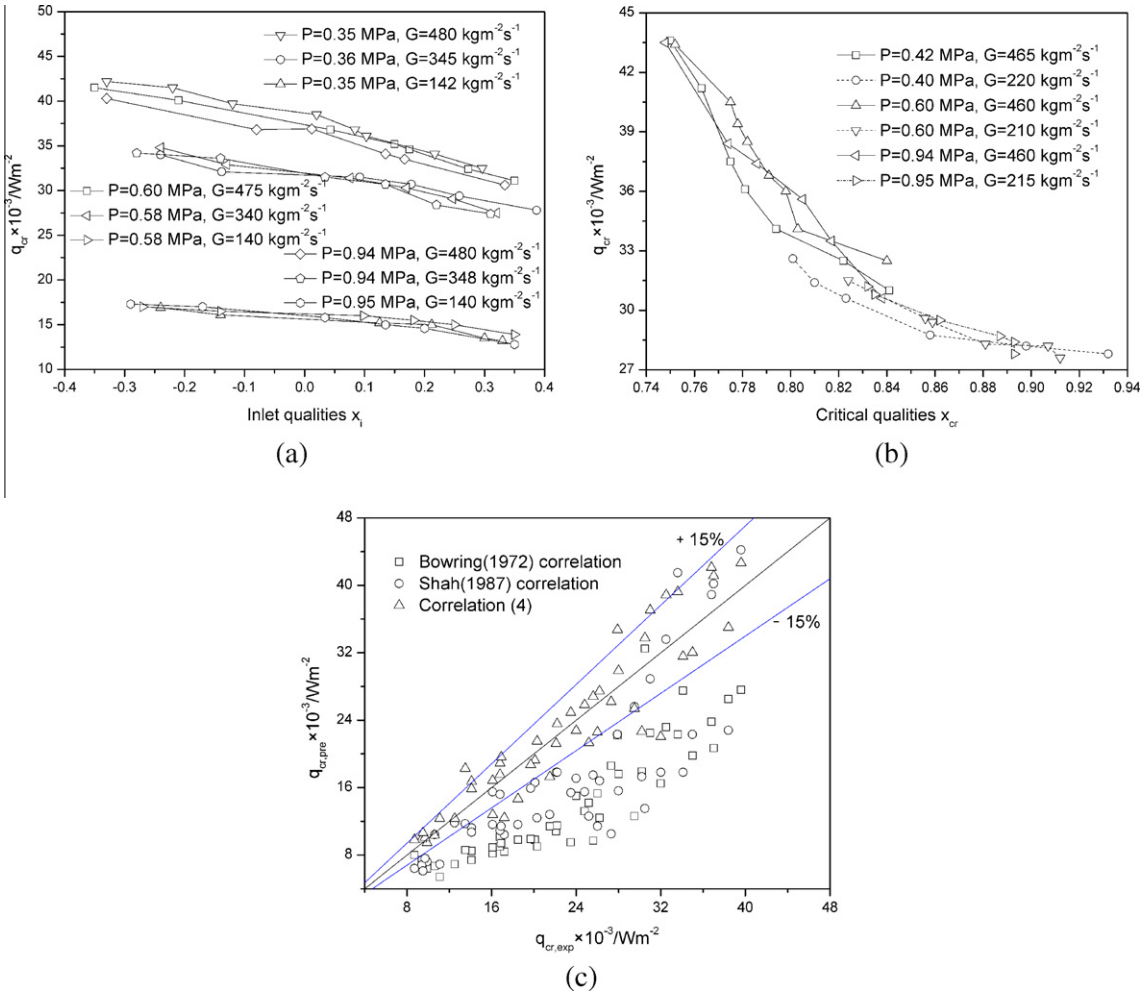

Fig. 4. Parametric effect on dry-out CHF and comparison of experimental data with classical correlations.

quality is lower, as shown in Fig. 3(d). This should be caused by intermittent rewetting of liquid phase remained in helically-coiled tube, which is synchronously affected by both gravity and centrifugal force, as well as the entrainment of rapid core gas flow.

3.3. Effect of system parameters on CHF

The parametric effect on CHF including inlet vapor quality, outlet pressure, mass flux and critical vapor quality, are shown in Fig. 4(a) and (b).

CHF values have an approximately linearly declining trend with increasing inlet vapor qualities, especially for high mass fluxes, and the regularity maintains at different pressures and mass fluxes, as shown in Fig. 4(a). It also shows that the outlet pressures do not seem to affect the CHF, and it seems like that CHF values decrease a little with increasing pressures at the same inlet vapor qualities and mass fluxes. While mass fluxed have more effect on CHF, and CHF values increases greatly with increasing mass fluxes at the same inlet vapor qualities and outlet pressures.

CHF values decrease with increasing critical vapor qualities. The critical vapor qualities at higher mass fluxes are lower than those at lower mass fluxes, as shown in Fig. 4(b). However, critical vapor qualities have a more obvious effect on CHF at higher mass fluxes, which is reflected in Fig. 4(b) based on the fact that generally the slopes of real lines (representing higher mass flux conditions) are bigger than those of broken lines (representing lower mass flux conditions).

3.4. Comparison with classical correlations

To evaluate the validity of Bowring [5] and Shah [7] correlations for CHF in helically-coiled tubes, experimental data were compared with the calculated results under the same conditions, as shown in Fig. 4(c). It is noted that the calculated values from the two correlations are both smaller than those of experiment results, with average errors of 40% and 35%, respectively. Actually, both can accurately predict CHF in straight tube, but not suitable for R134a CHF prediction in horizontal helically-coiled tubes under current experimental conditions.

Therefore, based on current experimental data, a new correlation for estimating R134a CHF in horizontal helically-coiled tubes is developed as follows with an error of ±15%, as shown in Fig. 4(c). This correlation was derived from the following parameter ranges: $0.30 < P < 0.95$ MPa, $60 < G < 500$ kg m^{-2} s^{-1}, $-0.36 < x_i < 0.35$ and $7.0 \times 10^3 < q_{cr} < 5.0 \times 10^4$ W m^{-2}.

$$\begin{aligned} B_o &= 1.135 \times 10^{-7}\ \mathrm{Re}^{2.32}\ D_n^{-2.5}\ N_d^{0.19}\ x_i^{-0.58} \\ B_o &= \frac{q_{cr}}{G\gamma}, \quad \mathrm{Re} = \frac{GD}{\mu} \\ D_n &= \mathrm{Re} \cdot \left(\frac{d_i}{D_c}\right)^{0.5}, \quad N_d = \frac{\rho_l}{\rho_g} \end{aligned} \tag{4}$$

4. Experimental uncertainties

The directly measured parameters in this study include length, temperature, pressure, mass flux, voltage and current. Based on the instructions of experimental equipment and calibration data sheets, the maximum uncertainty in measuring length and inner diameter of test section are ±0.054% and ±0.24%, respectively; the maximum uncertainty in measuring temperature is ±0.5%; the maximum uncertainty in measuring pressure is ±1.3%; the maximum uncertainty in measuring mass flux is ±2.1%; the maximum uncertainty in measuring voltage and current are ±1.8% and ±1.6%, respectively. Thus, the maximum uncertainty in measuring the heated area of test tube and critical heat flux value are about ±0.25% and ±2.4%, respectively, according to Moffat's experiment error transfer procedure [22].

5. Conclusions

Experiments for dry-out CHF in horizontal helically-coiled tube have been conducted using alternative refrigerant R134a to achieve a new prediction correlation for applications. From the analysis of wall temperature distribution and parametric effect on CHF, conclusions can be drawn as follows.

(1) Dry-out CHF usually occurs at outlet sections near the end of the test tube, and it spreads to the whole section circumference immediately. The wall temperatures at the front and offside (270° and 90°) frequently are higher than those of the other two sides.
(2) When there is a high outlet vapor quality after the CHF occurs, all the wall temperatures in the steady dry-out area will sometimes rise smoothly or even decrease to some extent. On the contrary, when the outlet vapor quality is lower, the wall temperatures will fluctuate with pressure wave, which is caused by intermittent rewetting of liquid-phase remaining in helically-coiled tube as described in text.
(3) CHF values have an approximately linear decline trend with increasing inlet vapor qualities, and decrease with increasing critical vapor qualities, especially for high mass fluxes, while the CHF values increase much more with increasing mass fluxes. At the present range of experimental conditions, mass fluxes have the most effect on CHF enhancement, while pressures have the least.
(4) Compared to experimental data, both Bowring and Shah correlations are inapplicable for evaluating CHF in horizontal helically-coiled tubes. A new dimensionless correlation for current experimental conditions is developed with an error of ±15%.

Acknowledgements

This work was supported by The National Natural Science Foundation of China (No. 50776055) and The Specialized Research Fund for the Doctoral Program of Higher Education of China (No. 20090131110035). Dr. Tien-Chien Jen would also like to acknowledge partial financial support from EPA (USA) award RD 833357.

References

[1] J.G. Collier, J.R. Thome, Convective Boiling and Condensation, third ed., Claredon Press, Oxford, England, 1994. pp. 329–365.
[2] S.Y. Ahmad, Fluid to fluid modeling of critical heat flux: A compensated distortion model, Int. J. Heat Mass Transfer 16 (3) (1973) 641–662.
[3] D.C. Groeneveld, J.Q. Shan, A.Z. Vasic, et al., The 2006 CHF look-up table, Nucl. Eng. Des. 273 (15–17) (2007) 1909–1922.
[4] N. Vaziri, A. Hojabri, A. Erfani, et al., Critical heat flux prediction by using radial basis function and multilayer perceptron neural networks: a comparison study, Nucl. Eng. Des. 237 (4) (2007) 377–385.
[5] R.W. Bowring, A simple but accurate round tube uniform heat flux, dry-out correlation over the pressure range, 0.7–12 MN/m^2 (100–2500 psia), Br. Report, AEEW-R789, Atomic Energy Establishment of Winfrith, Winfrith, U.K., 1972.
[6] Y. Katto, H. Ohno, An improved version of the generalized correlation of critical heat flux for the forced convective boiling in uniformly heated vertical tubes, Int. J. Heat Mass Transfer 27 (9) (1984) 1641–1648.
[7] M.M. Shah, Improved general correlation for critical heat flux during upflow in uniformly heated vertical tubes, Int. J. Heat Fluid Flow 8 (4) (1987) 325–335.
[8] Y.L. Wong, D.C. Groeneveld, S.C. Cheng, CHF prediction for horizontal tubes, Int. J. Multiphase Flow 16 (1) (1990) 123–138.
[9] R.M. Tain, S.C. Cheng, D.C. Groeneveld, Critical heat flux measurements in a round tube for CFCs and CFC alternatives, Int. J. Heat Mass Transfer 36 (8) (1993) 2049–3039.

[10] H.C. Kim, W.P. Bark, S.H. Chang, Critical heat flux of water in vertical round tubes at low pressure and low flow conditions, Nucl. Eng. Des. 199 (1–2) (2000) 49–73.
[11] I.L. Pioro, D.C. Groeneveld, S.C. Cheng, et al., Comparison of CHF measurements in R-134a cooled tubes and the water CHF look-up table, Int. J. Heat Mass Transfer 44 (1) (2001) 73–88.
[12] C.H. Kim, S.H. Chang, CHF characteristics of R-134a flowing upward in uniformly heated vertical tube, Int. J. Heat Mass Transfer 48 (11) (2005) 2242–2249.
[13] R. Sindhuja, A.R. Balakrishnan, S.S. Murthy, Critical heat flux of R-407c in upflow boiling in a vertical pipe, Appl. Therm. Eng. 28 (8-9) (2008) 1058–1065.
[14] C.H. Lee, I. Mudawar, A mechanistic critical heat flux model for subcooled flow boiling based on local upflow conditions, Int. J. Multiphase Flow 14 (6) (1988) 711–728.
[15] D.H. Hwang, W.P. Baek, S.H. Chang, Development of a bundle correction method and its application to predicting CHF in rod bundles, Nucl. Eng. Des. 139 (2) (1993) 205–220.
[16] X. Cheng, U. Müller, Critical heat flux and turbulent mixing in hexagonal tight rod bundles, Int. J. Multiphase Flow 24 (8) (1998) 1245–1263.
[17] I.L. Pioro, S.C. Cheng, A.Z. Vasic, et al., Some problems for bundle CHF prediction based on CHF measurements in simple flow geometries, Nucl. Eng. Des. 201 (2-3) (2000) 189–207.
[18] J. Chen, J.R. Liao, B. Kuang, et al., Fluid-to-fluid modeling of critical heat flux in 4×4 rod bundles, Nucl. Eng. Des. 232 (1) (2004) 47–55.
[19] N.I. Kolev, Check of the 2005 look-up table for prediction of CHF in bundles, Nucl. Eng. Des. 237 (9) (2007) 978–981.
[20] L.J. Guo, Dynamic characteristics of vapor/gas-liquid two phase flow in horizontal helically-coiled tubes, Ph.D. thesis, Xi'an Jiaotong University, Xi'an, China, 1989.
[21] D.C. Grocheveld, G.G.J. Delorme, Prediction of thermal non-equilibrium in the post dry-out regime, Nucl. Eng. Des. 36 (1) (1976) 17–26.
[22] R.J. Moffat, Describing the uncertainties in experimental results, Exp. Therm. Fluid Sci. 1 (1) (1988) 3–17.